A Novel Modulation for IoT: PSK-LoRa

Roberto Bomfin[†], Marwa Chafii[⋆] and Gerhard Fettweis[‡], *Fellow, IEEE*
Vodafone Chair Mobile Communication Systems, Technische Universität Dresden, Germany[†‡]
ETIS, UMR 8051, Université Paris-Seine, Université Cergy-Pontoise, ENSEA, CNRS, France[⋆]
roberto.bomfin@ifn.et.tu-dresden.de[†], marwa.chafii@ensea.fr[⋆] and gerhard.fettweis@tu-dresden.de[‡]

***Abstract*—This paper addresses the energy consumption concern of LPWAN by proposing an extension for the LoRa modulation. Conventional LoRa encodes data in the frequency-shift of a chirp, our extension consists in encoding additional data in the phase-shift using the PSK modulation, giving rise to the PSK-LoRa. Our motivation is to encode more data per unit of time without performance degradation, such that we have a more energy efficient system. In order to assess the performance of PSK-LoRa, we derive approximate bit error rate and packet error rate expressions, and then we compare against simulation. For instance, both analytical and numerical outcomes demonstrate that QPSK-LoRa has no performance loss in comparison to LoRa, indicating the feasibility of the new scheme.**

***Index Terms*—Chirp, IoT, LoRa, PSK.**

I. Introduction

The Internet-of-Things (IoT) communication systems have gained enormous attention in the past years. Basically, IoT allows a massive deployment of sensors to collect and process all sorts of data, therefore creating opportunities for a vast range of new applications [1]. With this new technology, the number of devices is expected to reach 50 billions connected devices by 2020 [2]. Naturally, the deployment of this unprecedentedly large number of devices bring challenges in all levels of a communication system. For instance, IoT devices are supposed to be cheap and to last for more than ten years, which means that IoT communications are constrained by hardware complexity and energy consumption. Thus, low-power wide area networks (LPWAN) protocols have emerged to fulfill these IoT requirements, offering a large area coverage and low energy consumption at the same time [3].

In this context, long-range wide area network (LoRaWAN) [4] has been proposed as a specification for LPWAN, becoming very popular commercially. The Long-Range (LoRa) modulation is the underlying physical layer based on a chirp spread spectrum technique [5]. LoRa has been described mathematically in [6] as the frequency shift chirp modulation (FSCM), showing that FSCM is more robust under frequency-selective channel than the frequency shift keying (FSK) modulation. Additionally, the authors of [7] provided approximated bit error rate (BER) curves for LoRa, since the exact ones are computationally intractable.

In this paper, we aim at extending LoRa and the work done in the aforementioned references [6], [7] in different ways. 1) In addition to encode data in the frequency-shift (FS), the PSK-LoRa system is proposed where information is also encoded in the phase-shift (PS) using the phase-shift keying (PSK) modulation. 2) Approximate closed-form expressions for BER and packet error rate (PER) for the additive white Gaussian noise (AWGN) channel are provided, whereas only closed-form curves of BER are developed for Rayleigh flat fading channel. The results of this work show that the additional information encoded in the phase-shift cause no significant performance loss for low modulation orders. The benefit of PSK-LoRa can be exploited in two ways, i) the total transmission duration can be decreased in order to decrease energy consumption, and ii) the code rate can be decreased in order to increase robustness of the coding scheme, meaning that the new modulation could operate in a lower signal-to-noise ratio region, therefore saving energy. 3) We provide a model with variable chirp rate normalized to the bandwidth, which provides a proper chirp rate and allows to model a system where data is also encoded in the chirp rate. 4) At the receiver side, we formally describe the fast Fourier transform (FFT)-based receiver model, which was used in [8] and is equivalent to the one in [6], [7].

The rest of the paper is organized as follows. In Section II we describe the proposed system model including i) single chirp transmission, ii) receiver and iii) packet transmission. In Section III, the derivations of the BER and PER expressions are provided for different channels. Numerical evaluations are presented and compared with analytical expressions in Section IV. And finally, Section V concludes the paper.

II. System Model

A. Single Chirp Transmission

LoRa employs a set of $2^{N_{\mathrm{F}}}$ orthogonal linear chirps and can be regarded as chirp-frequency-shift modulation [6], where N_{F}[1] stands for the amount of bits encoded in the frequency-shift (FS), $\mathbf{b}_{\mathrm{F}} \in \{0,1\}^{N_{\mathrm{F}}}$. Let $N_{\mathrm{F}} \in \{7,...,12\}$, which is equivalent to the spreading factor parameter [6]. $\mathbf{b}_{\mathrm{F}}$ is mapped into a symbol $k_{\mathrm{F}} \in \left\{0,1,2,...,2^{N_{\mathrm{F}}}-1\right\}$. In addition to N_{F} bits of the LoRa system, we propose to encode additional N_{P} bits in the phase of the transmitted signal according to the PSK modulation. We call the resulting modulation PSK-LoRa. Analogously, the bits to be encoded in the phase-shift (PS), $\mathbf{b}_{\mathrm{P}} \in \{0,1\}^{N_{\mathrm{P}}}$, are mapped to $k_{\mathrm{P}} \in \left\{0,1,2,...,2^{N_{\mathrm{P}}}-1\right\}$. Thus, this system carries in total $N_{\mathrm{F}}+N_{\mathrm{P}}$ bits per transmitted chirp as $\mathbf{b} = \{\mathbf{b}_{\mathrm{F}}, \mathbf{b}_{\mathrm{P}}\} \in \{0,1\}^{N_{\mathrm{F}}+N_{\mathrm{P}}}$. Hereafter, we provide systematic analysis on the advantages and disadvantages of the proposed PSK-LoRa design.

In this paper, we target at providing a general model that considers a proper chirp rate. For this purpose, we start by

[1]In this paper, we define the LoRa spreading factor as N_{F} for the sake of notational clearness, since we will also define N_{P} which stands for the number of bits encoded in the phase-shift.

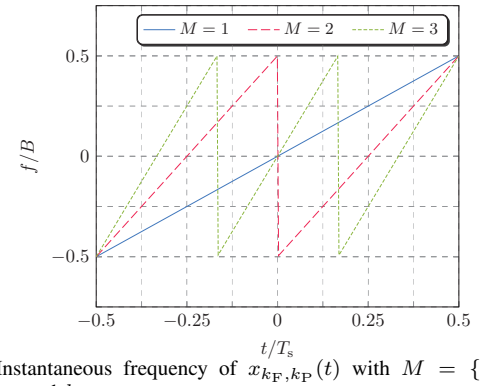

Fig. 1. Instantaneous frequency of $x_{k_\mathrm{F},k_\mathrm{P}}(t)$ with $M = \{1, 2, 3\}$ for arbitrary k_F and k_P.

defining the transmitted signal of a particular symbol $\{k_\mathrm{F}, k_\mathrm{P}\}$ in continuous-time domain as

$$x_{k_\mathrm{F},k_\mathrm{P}}(t) = \sqrt{\frac{E_\mathrm{s}}{T_\mathrm{s}}}\exp\big(j\pi(at^2 + 2b(k_\mathrm{F})t + c(k_\mathrm{P})\big), \quad (1)$$

for $-T_\mathrm{s}/2 \leq t \leq T_\mathrm{s}/2$ and zero otherwise, where T_s is the symbol duration in time. E_s is the energy per symbol, a is the chirp rate in Hz/s, $b(k_\mathrm{F})$ is the FS depending on k_F, and $c(k_\mathrm{P})$ is a phase rotation according to k_P. In LoRa, $c(k_\mathrm{P})$ can be dependent on k_F to guarantee phase continuity [5]. However, in this paper we use it to carry information of additional bits. The instantaneous frequency of (1) is

$$v(t) = \frac{1}{2\pi}\frac{d}{dt}\pi\left(at^2 + 2b(k_\mathrm{F})t + c(k_\mathrm{P})\right) = at. \quad (2)$$

With (2), we define the frequency range covered by the chirp as $v(T_\mathrm{s}/2) - v(-T_\mathrm{s}/2) = MB$, where B is the bandwidth and M is the amount of times that the chirp wraps around the spectrum, in which the frequency components above $1/2B$ wraps around starting from $-1/2B$ and vice-versa, as shown in Fig. 1 [2]. We define M for two reasons, i) our model allows the selection of a chirp rate that follows the patent of LoRa [5] by setting $M = 1$, while the authors [6], [7] implicitly assumed $M = 2$, and ii) we provide a general model that allows data to be encoded also in the chirp rate by making M depending on data. In addition, $v(T_\mathrm{s}/2) - v(-T_\mathrm{s}/2) = MB$ implies that the chirp rate is $a = MB/T_\mathrm{s}$. Finally, the discrete-time chirp is the sampled version of (1) and is given in Appendix (A) as

$$x_{k_\mathrm{F},k_\mathrm{P}}[n] = \sqrt{\frac{E_\mathrm{s}}{N}}\exp\left(j\pi\left(M\frac{n^2}{N} + \frac{2nk_\mathrm{F}}{N} + \frac{2k_\mathrm{P}}{2^{N_\mathrm{P}}}\right)\right), \quad (3)$$

for $n = \{0, 1, 2, ..., N-1\}$ and zero otherwise. In this paper we will always use $M = 1$ in order to follow [5]. Additionally, we highlight that practical studies have shown that current LoRa implementation uses $M = 1$ [8]. Appendix (B) shows that [6] and [7] implicitly assume $M = 2$. Alternatively, in case of higher sampling rate than B or implementation based on analog devices, the signal occupies greater bandwidth than B.

[2]Notice that the chirps in Fig. 1 for $M > 1$ assume a digital signal processing implementation of the transmitted signal with sampling rate equal to B. If the signal in (1) is sampled with higher sampling rate than B or is implemented with analog devices, then the transmit signal exceeds $\pm B/2$.

B. Single Chirp Receiver

The discrete-time received signal after synchronization and equalization is given by

$$r[n] = \sqrt{h}x_{k_\mathrm{F},k_\mathrm{P}}[n] + w[n], \quad (4)$$

where $\sqrt{h}$ is the magnitude of fading channel coefficient and $w[n]$ is the AWGN with zero mean and variance equal to σ^2. The detection is then performed in two steps, i) first estimate k_F using an FFT-based receiver which is equivalent to the one presented in [6], and ii) estimate k_P assuming that the transmitted chirp has an FS according to $\hat{k}_\mathrm{F}$.

First, the FS estimation is realized using the discrete Fourier transform (DFT) as

$$\begin{aligned} R[\nu] &= \frac{1}{\sqrt{N}}\sum_{n=0}^{N-1}\tilde{r}[n]\exp\left(-j2\pi\frac{n\nu}{N}\right) \\ &= \begin{cases} \sqrt{hE_\mathrm{s}}\exp\left(j2\pi\frac{k_\mathrm{P}}{2^{N_\mathrm{P}}}\right) + \phi[\nu] & \nu = k_\mathrm{F} \\ \phi[\nu] & \nu \neq k_\mathrm{F} \end{cases}, \end{aligned} \quad (5)$$

for $\nu = \{0, 1, 2, ..., N-1\}$, where $\tilde{r}[n] = r[n]\exp\left(-j2\pi Mn^2/N\right)$ is the received signal after being de-chirped. Also, the noise related terms $\phi[\nu]$ represent uncorrelated Gaussian samples with zero mean and variance equal to σ^2. Then, the FS is estimated as [7]

$$\hat{k}_\mathrm{F} = \arg_\nu \max(|R[\nu]|), \quad (6)$$

in which $|\cdot|$ returns the absolute value of its argument. We highlight that this procedure is more relevant from the implementation point of view, since it is more efficient computationally to perform the DFT instead of the correlation with all possible chirps. Subsequently, the PS estimate $\hat{k}_\mathrm{P}$ is obtained by applying the maximum likelihood (ML) PSK estimator to $R[\hat{k}_\mathrm{F}]$ [9].

It is important to comment that in this paper we assume a coherent system, i.e., the channel's phase rotation is compensated. It means that it is possible to estimate $\hat{k}_\mathrm{F}$ and $\hat{k}_\mathrm{P}$ jointly using the ML estimator, which would lead to a better or equal performance than the one using (6). However the ML detection is not explored in this work.

C. Packet Transmission

Neglecting the preamble and header for the sake of simplicity [10], the packet transmission is a concatenation of $N_\mathrm{c} = \lceil N_\mathrm{bits}/(N_\mathrm{F} + N_\mathrm{P})\rceil$ chirps, $\lceil\cdot\rceil$ being the ceil operator, and N_bits the total amount of payload bits. Notice that the necessary quantity of transmitted chirps decreases as N_P increases, meaning that PSK-LoRa consumes less energy transmission than LoRa. This aspect will be commented in Secion IV.

The packet transmission is expressed as

$$x[n] = \sum_{l=0}^{N_\mathrm{c}-1} x_{\mathbf{k}_\mathrm{F}[l],\mathbf{k}_\mathrm{P}[l]}[n - lN], \quad (7)$$

where $\mathbf{k}_\mathrm{F} = \{\mathbf{k}_\mathrm{F}[0], ..., \mathbf{k}_\mathrm{F}[N_\mathrm{c}-1]\}$ and $\mathbf{k}_\mathrm{P} = \{\mathbf{k}_\mathrm{P}[0], ..., \mathbf{k}_\mathrm{P}[N_\mathrm{c}-1]\}$ are the total symbols to be encoded in the FS and PS, respectively.

Under the assumption of perfect synchronization and channel estimation, the packet can be detected by applying the receiver in (6) for each chirp separately and then by properly concatenating the estimated bits.

III. Approximate BER and PER for Uncoded System

A. Closed-Form Expressions for AWGN Channel

In the AWGN channel, we simply set $\sqrt{h}$ in (4) as 1. The approximate symbol error rate (SER) for LoRa is already provided in [7] as

$$P_{\mathrm{s_F}} \approx Q\left(\frac{\sqrt{\Gamma N} - \left(H_{N-1}^2 - \frac{\pi^2}{12}\right)^{\frac{1}{4}}}{\sqrt{H_{N-1} - \left(H_{N-1}^2 - \frac{\pi^2}{12}\right)^{\frac{1}{2}} + \frac{1}{2}}}\right), \tag{8}$$

where $Q(z) = \frac{1}{2\pi}\int_z^\infty \exp(-u^2)du$ is the well known Q-function, $H_m = \sum_{i=1}^{m} 1/i$ is the mth harmonic number and $\Gamma = E_{\mathrm{s}}/(N\sigma^2)$ is the signal-to-noise ratio (SNR). At high SNR, the SER for the PSK modulation can be approximated by [9]

$$P_{\mathrm{s_P}} \approx 2Q\left(\sqrt{2\Gamma N}\sin\left(\frac{\pi}{2^{N_{\mathrm{P}}}}\right)\right). \tag{9}$$

Combining the SER equations $P_{\mathrm{s_F}}$ and $P_{\mathrm{s_P}}$ above, we obtain the BER for the PSK-LoRa model as

$$P_{\mathrm{b_{FP}}} \approx \frac{1}{2}P_{\mathrm{s_F}} + \frac{1 - P_{\mathrm{s_F}}}{N_{\mathrm{F}} + N_{\mathrm{P}}}P_{\mathrm{s_P}}, \tag{10}$$

where the first term $1/2P_{\mathrm{s_F}}$ results from the fact that whenever the FS is estimated wrong, both bits streams encoded in the FS and PS will have half of their bits estimated wrongly on average. Notice that for PSK symbol, this case is equivalent to a system with zero SNR. The second term is basically the average BER when the frequency-shift is estimated correctly with probability $1 - P_{\mathrm{s_F}}$, where we assumed that i) the FS and PS symbols are independent, and ii) that the variance of the noise component of $R[\hat{k}_{\mathrm{F}}]$ in (5) does not change under correct decision of $\hat{k}_{\mathrm{F}}$. Finally, the denominator results from the fact that only one bit out of $N_{\mathrm{F}} + N_{\mathrm{P}}$ is wrong on average, since we consider a PSK modulation respecting the gray mapping. One direct observation to be done on equation (10) is that if $P_{\mathrm{s_P}} \ll P_{\mathrm{s_F}}$, then $P_{\mathrm{b}} \approx P_{\mathrm{s_F}}/2$, meaning that the addition of extra bits will cause no significant performance loss.

Another relevant performance metric is the packet error rate (PER). For the LoRa system, the PER is expressed as

$$P'_{\mathrm{F}} \approx 1 - (1 - P_{\mathrm{s_F}})^{N_{\mathrm{c}}}, \tag{11}$$

where $1 - P_{\mathrm{s_F}}$ is the probability of a FS symbol being estimated correctly. The N_{c}th power indicates that the FS symbols are independent. For PSK-LoRa model, the PER is given by

$$P'_{\mathrm{FP}} \approx 1 - ((1 - P_{\mathrm{s_F}})(1 - P_{\mathrm{s_P}}))^{N_{\mathrm{c}}}, \tag{12}$$

where $(1 - P_{\mathrm{s_F}})(1 - P_{\mathrm{s_P}})$ is the probability that both FS and PS symbols are estimated correctly under a single chirp transmission. Again, the N_{c}th power indicates that the symbols are independent.

B. Closed-Form BER for Rayleigh Fading Channel

In this case, $\sqrt{h}$ is a Rayleigh random variable, therefore h follows a Chi-square distribution with one degree of freedom and with an expected normalized channel power of 1. Thus its probability density function is $f_h(\alpha) = \exp(-\alpha)$. The approximate SER of the LoRa system is [7]

$$P_{\mathrm{s_F}}^{\mathrm{rayl}} \approx Q\left(-\sqrt{2H_{N-1}}\right) - \sqrt{\frac{\Gamma N}{\Gamma N + 1}}\exp\left(\frac{2H_{N-1}}{2(\Gamma N + 1)}\right) \times Q\left(\sqrt{\frac{\Gamma N + 1}{\Gamma N}}\left(-\sqrt{2H_{N-1}} + \sqrt{\frac{2H_{N-1}}{\Gamma N + 1}}\right)\right). \tag{13}$$

The SER related to the PSK modulation can be approximated to [9]

$$P_{\mathrm{s_P}}^{\mathrm{rayl}} \approx 1 - \sqrt{\frac{\Gamma N}{\Gamma N + 1}}\sin\left(\frac{\pi}{2^{N_{\mathrm{P}}}}\right). \tag{14}$$

Using the AWGN related procedure, the PSK-LoRa BER under Rayleigh channel is given by Appendix C as

$$P_{\mathrm{b_{FP}}}^{\mathrm{rayl}} \approx \frac{1}{2}P_{\mathrm{s_F}}^{\mathrm{rayl}} + \frac{P_{\mathrm{s_P}}^{\mathrm{rayl}}}{N_{\mathrm{F}} + N_{\mathrm{P}}}, \tag{15}$$

Under the assumption that the channel coefficient is invariant during the whole packet transmission, the PER for the LoRa system is formulated as

$$P_{\mathrm{F}}^{'\mathrm{rayl}} \approx 1 - \int_0^\infty (1 - Q(\sqrt{2\alpha\Gamma N} - \sqrt{2H_{N-1}}))^{N_{\mathrm{c}}} e^{-\alpha} d\alpha, \tag{16}$$

which was obtained analogously to ([7], Eq. (28)). For PSK-LoRa model, the related expression is

$$P_{\mathrm{FP}}^{'\mathrm{rayl}} \approx 1 - \int_0^\infty (1 - Q(\sqrt{2\alpha\Gamma N} - \sqrt{2H_{N-1}}))^{N_{\mathrm{c}}} \left(1 - 2Q\left(\sqrt{2\alpha\Gamma N}\sin\left(\frac{\pi}{2^{N_{\mathrm{P}}}}\right)\right)\right)^{N_{\mathrm{c}}} e^{-\alpha} d\alpha, \tag{17}$$

where we simply included the PSK related term given in (9). Further development of (16) and (17) to obtain more compact closed form expressions is not straightforward, we will then evaluate them numerically in the next section in order to be compared with simulation results.

IV. Numerical Evaluation and Discussion

In this section, we aim at i) comparing the theoretical expressions developed in the previous section with simulations, and ii) comparing the performance of the proposed PSK-LoRa against the conventional LoRa [6] for different N_{P}. We consider the spreading factor of $N_{\mathrm{F}} = 10$ for all curves and $N_{\mathrm{P}} = \{2, 3, 4\}$ for the new system, implying in QPSK, 8PSK and 16PSK modulations, respectively. We purposely omit the results for $N_{\mathrm{P}} = 1$ (BPSK) since it performs as good as $N_{\mathrm{P}} = 2$. We consider $N_{\mathrm{bits}} = 320$, which results in $N_{\mathrm{c}} = \lceil N_{\mathrm{bits}}/N_{\mathrm{F}} \rceil = 32$ for LoRa and $N_{\mathrm{c}} = \lceil N_{\mathrm{bits}}/(N_{\mathrm{F}} + N_{\mathrm{P}}) \rceil = \{27, 25, 23\}$ for PSK-LoRa.

The outcomes for AWGN channel are reported in Fig. 2. Firstly, we observe that the approximate BER and PER expressions satisfactorily match the simulation, meaning that

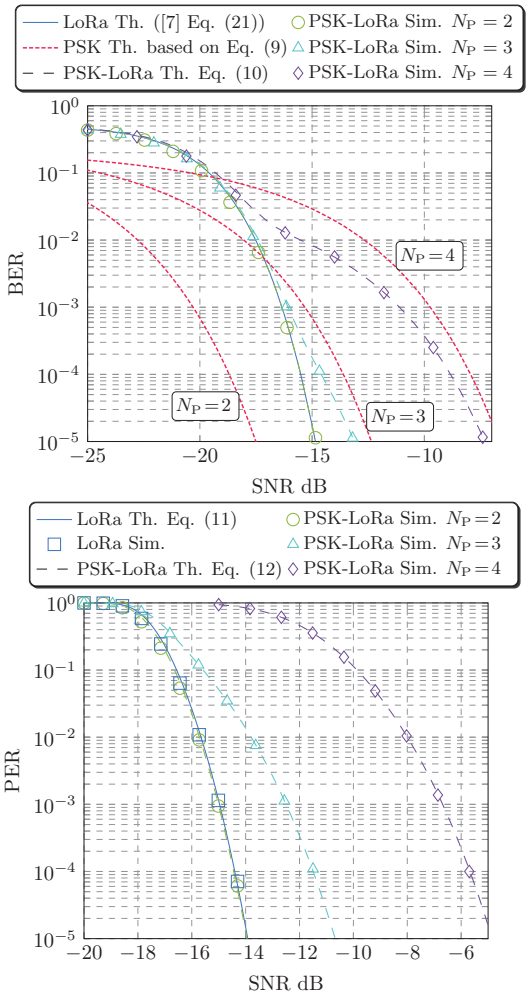

Fig. 2. BER and PER under AWGN channel.

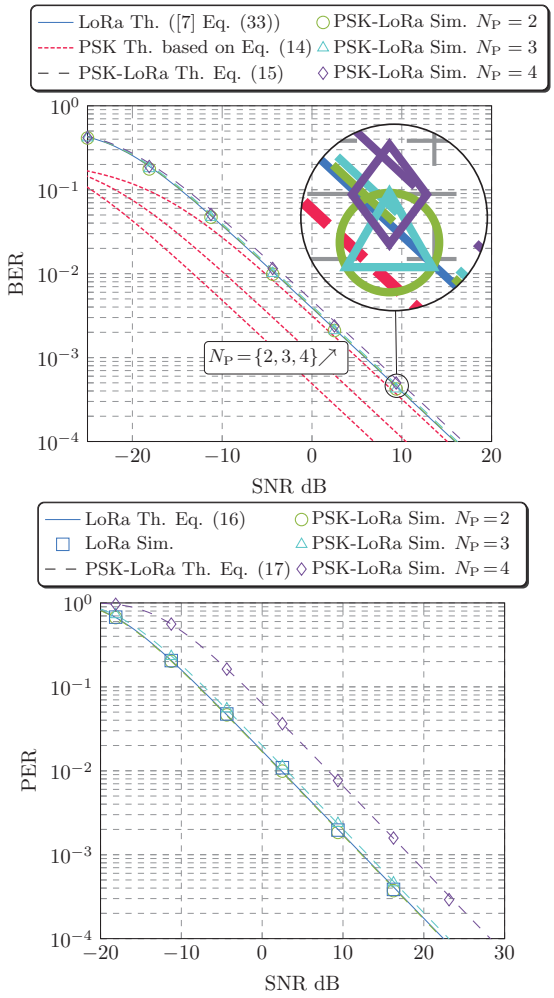

Fig. 3. BER and PER under Rayleigh channel.

they are indeed valid. Secondly, we notice that the proposed PSK-LoRa with $N_P = 2$ presents no performance loss in comparison to the original LoRa. In fact, there is a slight performance gain in terms of PER, which is justified due to smaller number of transmitted chirps, N_c. On the other hand, there is a considerable performance loss for $N_P = \{3, 4\}$, which happens due to the increase of BER related to the PSK modulation.

Figure 3 depicts the results for the Rayleigh channel. Regarding the accuracy of the theoretical curves, we observe that they are slightly above the simulation, which is expected since the same behavior was reported in ([7] Fig. 2). With respect to the performance, it is surprising that PSK-LoRa with $N_P = \{3, 4\}$ has very similar performance to $N_P = 2$ in terms of BER. This happens because the PSK component is less sensitive to fading than the LoRa one. Notice that all PSK curves are below LoRa. Nevertheless the performance in terms of PER increases the differences. In particular, $N_P = 4$ shows considerable degradation.

The results demonstrate the potential of the proposed PSK-LoRa scheme. In order to provide a basic analysis on the benefits of PSK-LoRa, consider that the frame structure of LoRa is composed by *preamble*, *header* and *payload (including optional CRC)* [10]. As long as the proposed system does not decrease the PER, the reduction of energy consumption of PSK-LoRa in comparison to LoRa can be formulated as

$$E_r = 1 - \frac{N_c^{\mathrm{Pr+He}} + \lceil N_{\mathrm{bits}}/(N_F + N_P) \rceil}{N_c^{\mathrm{Pr+He}} + \lceil N_{\mathrm{bits}}/N_F \rceil}, \qquad (18)$$

where $N_c^{\mathrm{Pr+He}}$ are the necessary amount of chirps for the preamble and the header using the conventional LoRa for simplicity. For instance, considering the system with $N_F = 10$, $N_P = 2$, $N_{\mathrm{bits}} = 320$, and assuming $N_c^{\mathrm{Pr+He}} = 18$ chirps, we have $E_r = 0.1$, which means that the proposed PSK-LoRa system consumes 10% less energy than conventional LoRa. Consequently, if a regular LoRa device can last for 10 years, the respective QPSK-LoRa would last 11 years maintaining the same performance. Also, it is worth noticing that if N_{bits} is too small, then increasing N_P will not produce a relevant impact since most of the energy is spent in the preamble and the header. Yet, another possibility to explore PSK-LoRa is to reduce the coding rate in order to improve robustness.

Finally, although the potential of the PSK-LoRa is clear, it also has some challenges. For instance, it may not satisfy phase continuity, which can be avoided in LoRa [5]. In addition, the new system relies in channel estimation in order to perform coherent PSK demodulation. This also means that PSK-LoRa is expected to suffer more than LoRa in mobile channels, since in this case the channel would impact more the bits encoded in the phase-shift. Thus, the limitations of

the proposed system with imperfect channel estimation and mobility scenario should be addressed.

V. Conclusion

This paper proposes an extension of LoRa modulation called PSK-LoRa. The new scheme encodes additional data in the phase of the transmitted chirps using the PSK modulation. Approximate expressions for bit error rate and packet error rate have been derived for the AWGN and the Rayleigh fading channels. In terms of performance, the results have undoubtedly demonstrated the potential of PSK-LoRa in comparison to LoRa, especially for low PSK modulation orders. Basically, PSK-LoRa can transmit the same amount of information as LoRa using less time resources with no performance loss in some cases. Therefore, LPWAN can benefit from this modulation in terms of energy consumption, which is a major concern for these systems.

Appendix A
Discrete-Time Signal

The respective discrete-time model of (1) has each sample at $T = 1/B$ seconds. Since LoRa defines $N = 2^{N_\mathrm{F}}$ orthogonal chirps, each discrete-time chirp should have at least N samples, thus we define $T_\mathrm{s} = NT$. Then, the discrete-time chirp carrying the symbol $\{k_\mathrm{F}, k_\mathrm{P}\}$ is

$$\begin{aligned}\tilde{x}_{k_\mathrm{F},k_\mathrm{P}}[n] &\overset{(a)}{=} x_{k_\mathrm{F},k_\mathrm{P}}(nT - T_\mathrm{s}/2)\\ &\overset{(b)}{=} \sqrt{\frac{E_\mathrm{s}}{N}}\exp\left(j\pi M\frac{(n-\frac{N}{2})^2}{N}\right)\\ &\quad\times\exp\left(2b(k_\mathrm{F})T\left(n-\frac{N}{2}\right)+c(k_\mathrm{P})\right)\\ &\overset{(c)}{=} \sqrt{\frac{E_\mathrm{s}}{N}}\exp\left(j\pi\left(M\frac{n^2}{N}+\frac{2nk_\mathrm{F}}{N}+\frac{2k_\mathrm{P}}{2^{N_\mathrm{P}}}\right)\right)\end{aligned} \tag{19}$$

for $n = \{0, 1, 2, ..., N-1\}$ and zero otherwise. (a) is due to $-T_\mathrm{s}/2 < t < T_\mathrm{s}/2$ and (b) is obtained by making $nT - T_\mathrm{s}/2 = T(n - N/2)$ and $a = MB/T_\mathrm{s} = M/(2^{N_\mathrm{F}}T^2)$. (c) is obtained by i) considering that the FS provoked by k_F must be multiple of $B/N = 1/(NT)$ to produce orthogonal sequences, we have $b(k_\mathrm{F}) = (k_\mathrm{F} - N/2)/(NT)$, where we consider minimum and maximum FS as $-B/2$ and $B/2$, respectively, and ii) making the PS a fraction of 2π according to the PSK modulation, which is realized with $c(k_\mathrm{P}) = 2k_\mathrm{P}/2^{N_\mathrm{P}} + k_\mathrm{F} - 3N/4$, where the terms $k_\mathrm{F} - 3N/4$ are simply a phase compensation such that (19) can be expressed in a clearer form.

Appendix B
Current LoRa Model

The LoRa chirps in [6], [7] is given by

$$\begin{aligned}x_{k_\mathrm{F}}[n] &\overset{(a)}{=} \sqrt{\frac{E_\mathrm{s}}{N}}\exp\left(j2\pi\left(k_\mathrm{F}+n\right)\bmod N\ \frac{n}{N}\right)\\ &\overset{(b)}{=} \sqrt{\frac{E_\mathrm{s}}{N}}\exp\left(j\pi\left(2\frac{n^2}{N}+\frac{2nk_\mathrm{F}}{N}\right)\right),\end{aligned} \tag{20}$$

where (a) is given by definition and (b) is obtained considering that $(k_\mathrm{F}+n) \bmod N$ is equivalent to $k_\mathrm{F}+n$, since $(k_\mathrm{F}+n) \bmod N = k_\mathrm{F}+n$ if $k_\mathrm{F}+n < N$ and $k_\mathrm{F}+n-N$ otherwise, where the term $-N$ will produce a rotation of $-2\pi n$ radians which is equivalent to 0 radians for all n. Clearly, $x_{k_\mathrm{F}}[n]$ in (20) is equal to $x_{k_\mathrm{F},k_\mathrm{P}}[n]$ in (19) with $M = 2$ and $k_\mathrm{P} = 0$.

Appendix C
PSK-LoRa BER under Rayleigh Channel

The BER for the PSK-LoRa under one channel realization is given by

$$\begin{aligned}P^{\mathrm{rayl}}_{\mathrm{b_{FP}}}(h) &\overset{(a)}{\approx} \frac{1}{2}P_{\mathrm{s_F}}(h) + \frac{1-P_{\mathrm{s_F}}(h)}{N_\mathrm{F}+N_\mathrm{P}}P_{\mathrm{s_P}}(h),\\ &\overset{(b)}{\approx} \frac{1}{2}P_{\mathrm{s_F}}(h) + \frac{P_{\mathrm{s_P}}(h)}{N_\mathrm{F}+N_\mathrm{P}}\end{aligned} \tag{21}$$

where (a) is obtained using (10), $P_{\mathrm{s_F}}(h) = Q\left(\sqrt{2h\Gamma N} - \sqrt{2H_{N-1}}\right)$ being the instantaneous LoRa SER formulated in the integral's argument of ([7], Eq. (28)), and $P_{\mathrm{s_P}}(h) = 2Q\left(\sqrt{2h\Gamma N}\sin\left(\pi/2^{N_\mathrm{P}}\right)\right)$ is (9) with instantaneous SNR equal to $h\Gamma N$. Step (b) simply neglects the product $P_{\mathrm{s_F}}(h)P_{\mathrm{s_P}}(h)$ because it will be orders of magnitude smaller than the other terms, causing no significant impact in the result. Finally, the approximated BER found by solving $\int_0^\infty P^{\mathrm{rayl}}_{\mathrm{b_{FP}}}(\alpha)\exp(-\alpha)d\alpha$ using the step (b), whose result is

$$P^{\mathrm{rayl}}_{\mathrm{b_{FP}}} \approx \frac{1}{2}P^{\mathrm{rayl}}_{\mathrm{s_F}} + \frac{P^{\mathrm{rayl}}_{\mathrm{s_P}}}{N_\mathrm{F}+N_\mathrm{P}}. \tag{22}$$

Acknowledgments

The computations were performed at the Center for Information Services and High Performance Computing (ZIH) at Technische Universität Dresden.

This work was supported by the European Union's Horizon 2020 under grant agreements no. 732174 (ORCA project) and no. 777137 (5GRANGE project).

References

[1] J. Gubbi, R. Buyyab, S. Marusica, and M. Palaniswamia, "Internet of Things (IoT): A vision, architectural elements, and future directions," *Future Generation Computer Systems*, vol. 29, no. 7, 2013.

[2] D. Evans, "The Internet of Things: How the Next Evolution of the Internet is Changing Everything," *Cisco InternetBusiness Solutions Group:* San Jose, CA, USA, 2011.

[3] U. Raza, P. Kulkarni, and M. Sooriyabandara, "Low power wide area networks: An overview," *IEEE Communications Surveys Tutorials*, vol. 19, pp. 855–873, Secondquarter 2017.

[4] "LoRaWAN Specification," *LoRa Alliance,* Inc, Jan. 2015, rev. 1.

[5] O. Seller and N. Sornin, "Low Power Long Range Transmitter," Aug 2014. US Patent 2014/0219329 A1.

[6] L. Vangelista, "Frequency Shift Chirp Modulation: The LoRa Modulation," *IEEE Signal Processing Letters*, vol. 24, pp. 1818–1821, Dec 2017.

[7] T. Elshabrawy and J. Robert, "Closed-Form Approximation of LoRa Modulation BER Performance," *IEEE Comm. Lett.*, vol. 22, pp. 1778–1781, Sept 2018.

[8] M. Knight and B. Seeber, "Decoding LoRa: Realizing a Modern LPWAN with SDR," *Proceedings of the GNU Radio Conference*, vol. 1, no. 1, 2016.

[9] A. Goldsmith, *Wireless Communications*. Cambridge University Press, 2005.

[10] A. Augustin, J. Yi, T. Clausen, and W. M. Townsley, "A Study of LoRa: Long Range and Low Power Networks for the Internet of Things," *Sensors*, vol. 16, no. 9, 2016.